Examples of Electron Microscopy Observations at Different Length Scales

Dominique Schryvers[1], Wim Tirry[1], Zhiqing Yang[1], Barbora Bartova[1], Silvia Ignacova[2], Shanshan Cao[1], Arvind Srivastava[1]

[1]Electron Microscopy for Materials Science (EMAT), University of Antwerp (UA), Groenenborgerlaan 171, B-2020 Antwerp, Belgium, nick.schryvers@ua.ac.be
[2]Institue of Physics, Academy of Sciences, Prague, 18221, Czech Republic

ABSTRACT

The present contribution will focus on recent transmission electron microscopy observations of structures at different length scales in materials undergoing phase transformations. The examples are chosen so as to provide links to possible mathematical models describing these features at their respective length scales. The latter range from the atomic scale when dealing with atomic structures over the nanoscale when looking at structural defects such as twin boundaries to the micron scale when talking about domain structures. An example of the first is the refinement of the atomic structure of the Ni_4Ti_3 precipitate formed in Ni-rich Ni-Ti alloys to enhance the shape memory behaviour, the 3D configuration of these precipitates an example of the last. Some other examples will be shown as well.

1. Introduction

When attempting to model real life structures or systems or situations the first aim should always be to reproduce existing cases that have been well documented by experiment. Only when a modeling environment stands the test of scrutiny against reality, one should think of applying the model to unknown situations that cannot be reproduced in the lab. In the present contribution we will present some examples of recently investigated real atomic or microstructures in solid state materials and of which the understanding could severely be improved by modeling on different length scales from the atomic to the continuum.

The experimental observations are in most cases performed with transmission electron microscope (TEM) instruments which enable magnifications up to a few million times with resolutions down to one tenth of a nanometer, i.e., well below the interatomic distances in most solids. The effective nature of the technique implies that one observes a sort of 2D transformation of the internal structure (not exactly a projection, but close) with the actual image also depending on the imaging conditions such as focus of the objective lens and thickness of the sample. The latter needs to be extremely small, i.e. at least below 100 nm and for some cases even below 10 nm, and for this special sample preparation techniques need to be applied. On one occasion, the result of a three-dimensional slice-and-view technique obtained with a dual-beam scanning electron microscope (SEM) plus focused ion beam (FIB) instrument will be discussed.

Although of course many different materials could be used as examples for the present purpose, alloy systems active in the field of shape memory or superelastic components are a very good candidate as aspects on many different length scales play important roles in these systems. Indeed, the physics (electronic structure, thermodynamics, …) of the stability of the high temperature austenite versus low temperature martensite basic lattice structures determines not only the symmetry of these structures but also the transformation temperatures and their dependencies on, e.g., composition. Here discrete atomic scale modeling (e.g., density functional theory (DFT)) can be relevant to unravel the influence of different parameters such as electron density or distribution and bonding on the stability of the different structures and thus on the displacive (and sometimes more complex) transformation processes. On the next level the symmetry of martensite dictates the number of variants and austenite-martensite and martensite-martensite interfaces which in its turn leads to a variety of microstructures that can be modeled by different, usually continuum level methods. Modeling can also be used to investigate the growth of precipitates in a matrix and of the effect of that precipitate on the surrounding matrix and in the present contribution we will primarily focus on examples involving precipitates in different shape memory alloys, with the focus on Ni-based systems.

2. Precipitation in NiTi

In the near-equiatomic NiTi system, which is often used for medical applications like stents and orthodontic wires [1] the crystal transforms from a cubic (B2) to a monoclinic (B19') phase. This transformation can occur upon cooling or under the influence of an applied stress, in which case large strains might be obtained that can be fully recovered without plastic deformation. The properties of this transformation such as transformation temperature, number of transformation steps and whether it is superelastic or not are strongly influenced by the presence of Ni_4Ti_3 precipitates [2]. These precipitates have an ordered crystal structure and occur in the matrix after an appropriate heat treatment. They are enriched in Ni and have an estimated Ni:Ti = 4:3 composition ratio. The structure of these precipitates was first proposed by Tadaki *et al.* to be rhombohedral with spacegroup R-3 [3]. A morphological study by the same authors reveals a lens shape with 8 orientation variants.

Fig 1a is a typical conventional TEM image of Ni_4Ti_3 lens shaped precipitates embedded in the matrix and oriented along different families of {111} planes. Depending on the annealing conditions (exact temperature and time) the precipitates will be larger and further apart or smaller and closer together. The particular lens shape of the precipitates is dictated by the contraction of the lattice in the direction perpendicular to the central plane of the disc of the lens. This contraction is made possible by the replacement of one Ti atom by one Ni atom and the subsequent reshuffling of atoms in the planes parallel to the central disc: Fig 1b shows a top view (i.e., looking down on the disc of the precipitate) of the refined structure revealing these shuffles. The latter was found by applying a novel technique of multi-slice least-squares optimization of electron diffraction intensities obtained from these nano-scaled precipitates [4]. Although this results from a relatively important composition change (i.e., with respect to the matrix) and although it implies a rather severe lattice change, only very small changes are observed in the fine structure of electron energy loss (so-called ELNES) spectra, which could be confirmed by density-of-states (DOS) calculations, indicating very little if any charge transfer at all [5]. The Young's modulus, on the other hand, does change considerably, as could be shown by measurements of the position of the maximum of the plasmon peak in the low loss part of the energy loss spectrum, as seen from fig 1c. Following the criterium designed by Oleshko and Howe [6] values of 124 GPa and 175 GPa for the matrix, respectively precipitate, were obtained [5], showing a much harder precipitate in comparison with the matrix.

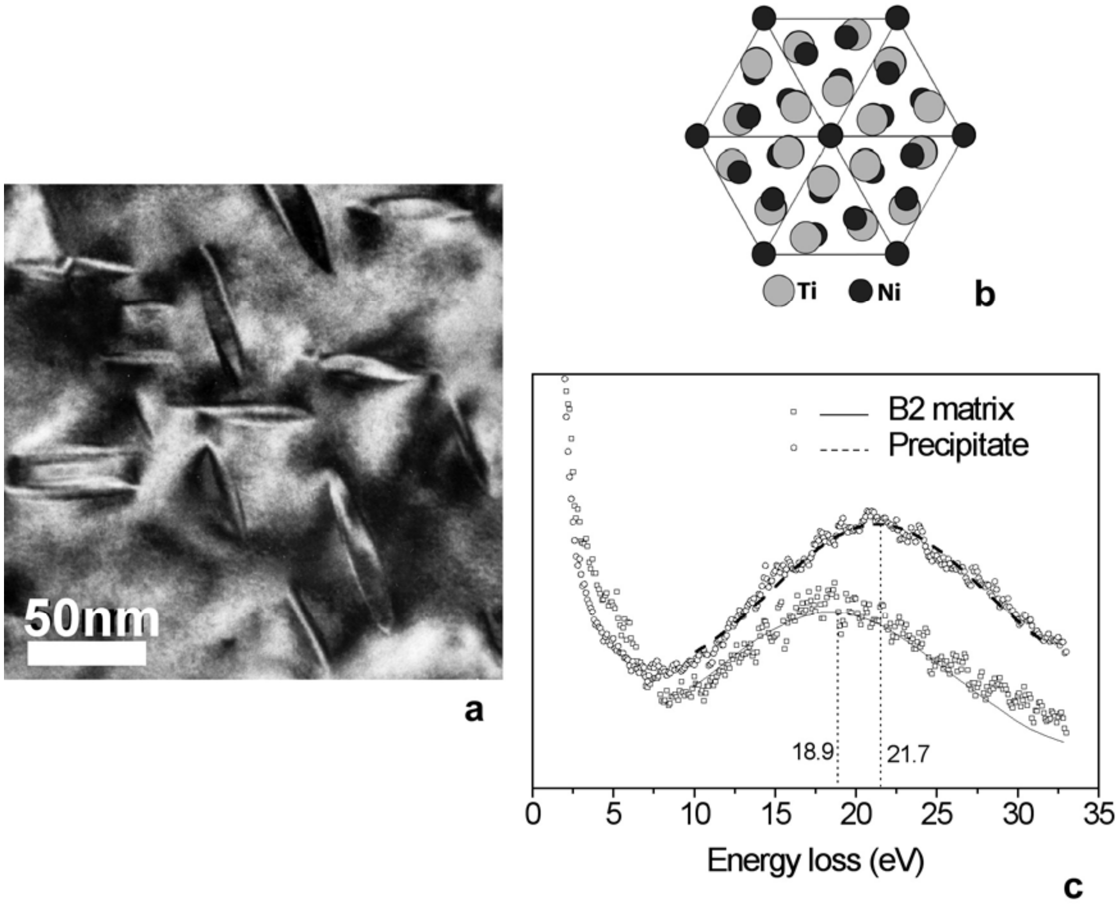

Figure 1. (a) Conventional TEM image of Ni_4Ti_3 lens shaped precipitates embedded in the NiTi matrix. (b) Projected structure of the refined structure of Ni_4Ti_3 in the $[111]_R$ direction. (c) Low loss part of the EELS spectrum showing the difference in the plasmon peaks between matrix and precipitate.

As a result of the contraction of the precipitate, the austenite matrix close by the central disc of the precipitate will be expanded (seen as strain contrast in fig 1a) which in turn will possibly affect the ensuing martensitic transformation when the material is cooled or strained. Moreover, the enrichment of Ni in the precipitate will decrease the Ni amount in the matrix in the vicinity of the precipitate and again this can have a profound influence on the martensitic transformation temperature [1]. So in order to gain insight into these different aspects of the growth of these precipitates we performed quantitative analyses of the strain and concentration gradients in the matrix surrounding the precipitates. Fig 2 shows a deformation gradient measured along the $[101]_{B2}$ direction of the NiTi matrix in between two nanoscale precipitates. The maximum deformation mounts to about 1.2% above the normal matrix lattice parameter (indicated by the horizontal dashed line in the graph on the right) and rapidly decreases after about 10 nm away from the precipitate-austenite interface. In between the precipitates there is a region of no deformation of about 20 nm. The measured deformation accounts for the total amount of strain necessary to accommodate the observed precipitates (when assuming a symmetric situation on either sides of the precipitates). These measurements were performed on high resolution images revealing the atomic lattices of the respective structures so that interplanar lattice spacings can directly or indirectly be measured [7].

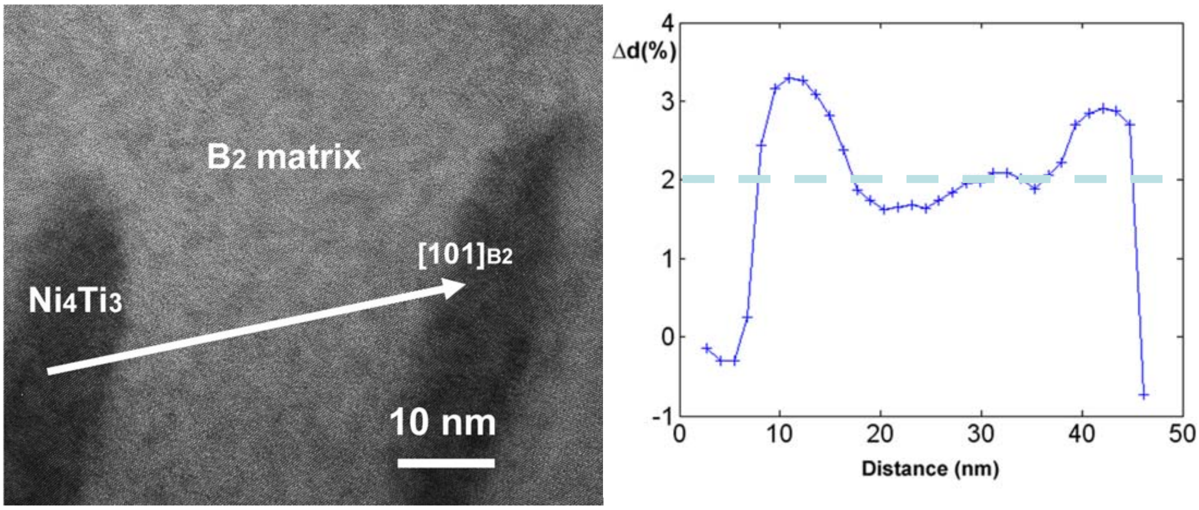

Figure 2. Deformation of the NiTi matrix as measured along the $[101]_{B2}$ direction between two small Ni_4Ti_3 precipitates

By performing spectroscopic measurements with nanoprobe or filtering techniques, concentration gradients revealing Ni depletion can be found. Regions between 10 and 150 nm wide, depending on the size of the precipitate, are depleted in Ni due to the Ni-enrichment of the precipitate: Ni/Ti ratios down to 0.94 instead of the nominal 1.04 of the matrix can be found in these areas. Again, quantification shows that these regions can provide all the Ni needed to form the precipitates [8]. For both strain and composition gradient cases, these new nanoscale quantifications may provide data that can allow for better modeling of the influence of the Ni_4Ti_3 precipitates on the martensitic transformation and thus the shape memory and superelastic behaviour of this material.

Although TEM imaging, diffraction and spectroscopy can provide a wealth of information on the structure and chemistry and electronic nature of the material, obtaining true three-dimensional information has always been a remaining challenge for microscopists working in micro- and nanoscale materials sciences. With recent evolutions of tomography, however, important steps have been taken to overcome technological as well as conceptual problems so that new results are appearing revealing the internal 3D nature of solid state materials. In fig 3 an example of again the same precipitates, but now allowed to grow much larger, is shown in which a first glance is presented into the volume configuration of these lens shapes. This result was obtained by the slice-and-view technique in which a three-dimensional bulk piece of material of NiTi containing relatively large Ni_4Ti_3 precipitates is sliced away by a focused ion beam with imaging by a scanning electron microscope after every slicing. The stack of images is then afterwards combined to form a 3D volume picture box from which different types of measurements such as volume fractions, relative orientations, cuttings, etc. can be obtained. From the present image it can, e.g., be seen that the precipitates can truly intersect, which is sometimes hard to conclude from 2D images. Of course these new possibilities for 3D imaging open new ways for interaction with modeling programs.

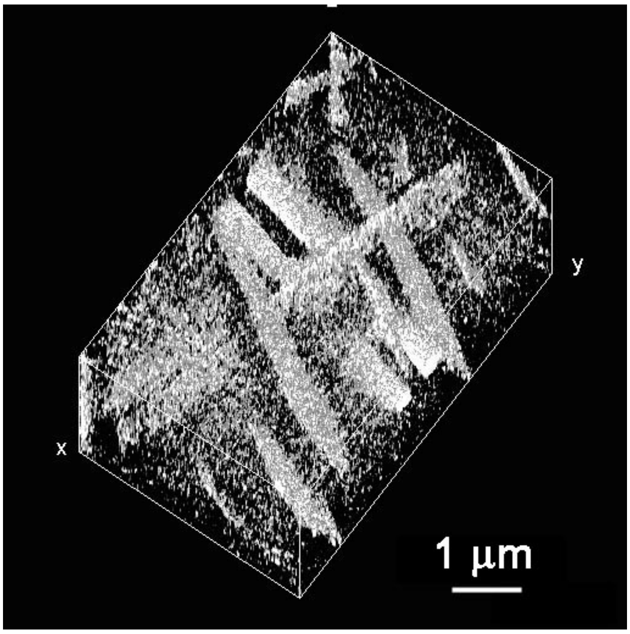

Figure 3. First 3D view of the Ni_4Ti_3 precipitates.

Instead of controlling the characteristics of the alloy by changing the composition or thermal treatment, thermomechanical treatments can even further improve the functional properties. Amongst these, low temperature annealing following appropriate cold deformation is one of the effective methods for controlling shape memory properties. Freshly rolled material shows texture of nanoscale grains and small amorphous bands in the rolling direction while in annealed material the texture is lost and the bands gradually crystallize above 400°C [9]. Further short annealing above 450°C produces Ti_2Ni precipitates while longer annealing above 500°C forms Ni_4Ti_3 precipitates. Annealing above 600°C produces Ni_3Ti_2 precipitates.

3. Precipitation in CoAlNi

Next to temperature and stress, in several novel shape memory alloys a magnetic field is used as a controlling factor of the martensitic transformation. One example is $Co_{38}Ni_{33}Al_{29}$ in which small Co rich fcc precipitates are observed in as-received material. Fig 4a shows an area with relatively large rod-like shaped precipitates with sizes about 23 nm in length and 14 nm in width. From electron diffraction it can be concluded that their crystallographic relation with the B2 matrix is of the Kurdjumov-Sachs type ($(110)_{b.c.c.}//(111)_{f.c.c.}$, $[-11-1]_{b.c.c.}//[-110]_{f.c.c.}$). Even smaller sphere-like precipitates are also observed in the same sample as seen from the high resolution image in fig 4b with fig 4c revealing the Co content in these precipitates obtained by energy filtered TEM. Again the distribution of these precipitates and their effects on the matrix will affect the martensitic transformation and thus the shape memory behaviour. Further detailed TEM investigations will provide more quantified data to exchange with modeling procedures.

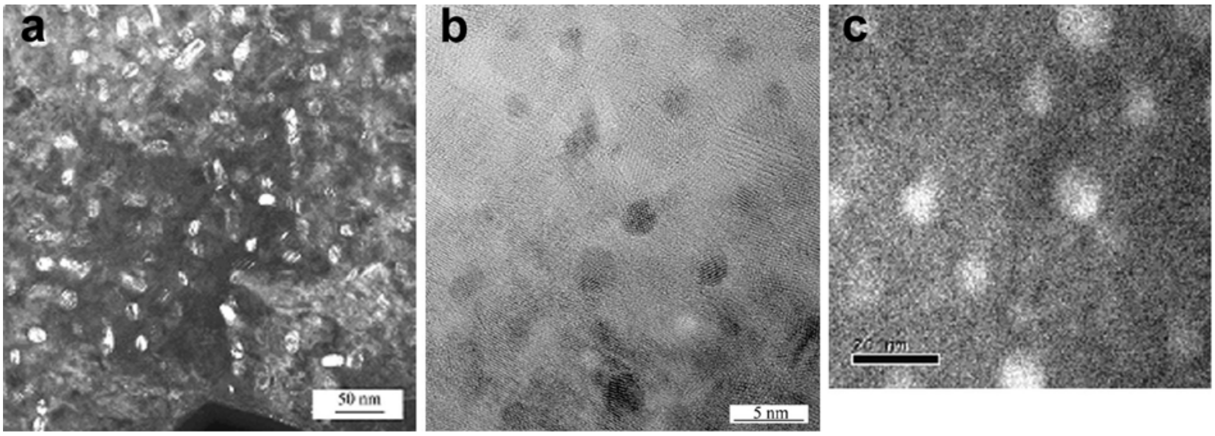

Figure 4. fcc Co rich precipitates with K-S relationship with the B2 matrix in as-received $Co_{38}Ni_{33}Al_{29}$: (a) rod-like shapes, (b) nano-spheres with (c) Co filtered image.

Acknowledgements

This work was made possible through financial support from a GOA project of the University of Antwerp on “Characterization of nanostructures by means of advanced EELS and EFTEM” a project of the National Science Foundation of Flanders on “The functional properties of shape memory alloys: a fundamental approach” and a Marie Curie Research Training Network on “Multi-scale modeling and characterization for phase transformations in advanced materials”.

References

1. K. Otsuka and X. Ren, “Physical Metallurgy of NiTi-based Shape Memory Alloys” Progress Mater. Sc. **50,** 511-678 (2005)
2. J. Khalil-Allafi, A. Dlouhy, and G. Eggeler, “Ni_4Ti_3-precipitation During Aging of NiTi Shape Memory Alloys and its Influence on Martensitic Phase transformations” Acta Mater. **50,** 4255-4274 (2002)
3. T. Tadaki, Y. Nakata, K. Shimizu, and K. Otsuka, “Crystal Structure, Composition and Morphology of a Precipitate in an Aged Ti-51at%Ni Shape Memory Alloy” JIM. **27,** 731-740 (1986)
4. W. Tirry, D. Schryvers, K. Jorissen, and D. Lamoen, “Electron diffraction structure refinement of Ni_4Ti_3 precipitates in $Ni_{52}Ti_{48}$“, Acta Cryst. (in press)
5. Z.Q. Yang and D. Schryvers, “Electron Energy-loss Spectroscopy Study of NiTi Shape Memory Alloys”, proc. ESOMAT 2006, Bochum, Germany, edited by G. Eggeler & E. Wassermann (to be published)
6. J.M. Howe and V.P. Oleshko, “Application of Valence Electron Energy-loss Spectroscopy and Plamon Energy Mapping for Determining Material Properties at the Nanoscale” Journal of Electron Microscopy, **53,** 339-351 (2004)
7. W. Tirry and D. Schryvers, “Quantitative Determination of Strain Fields Surrounding Ni_4Ti_3 Precipitates in NiTi” Acta Mater. **53,** 1041-1049 (2005)
8. Z.Q. Yang, W. Tirry, and D. Schryvers, “Analytical TEM Investigations on Concentration Gradients Surrounding Ni_4Ti_3 Precipitates in Ni-Ti Shape Memory Material” Scripta Mat. **52,** 1129-1134 (2005)
9. A.K. Srivastava, D. Schryvers, and J. Van Humbeeck, “TEM Studies on Cold-Rolled and annealed Ni-Ti Alloys” (to be published)